Direct Current Forcing of an Atmospheric Multiburner Flame for Rocket Combustor Emulation

Paulo R. Salvador* and Kunning G. Xu†
The University of Alabama in Huntsville, Huntsville, Alabama 35806

DOI: 10.2514/1.A33737

This study investigated the effect of direct current electric fields on the response of an atmospheric, premixed methane-air flame using electrode geometries intended to emulate a simplified liquid rocket engine combustion chamber. The burners consisted of single- and multielement configurations to determine the difference between element radial location and flame-to-flame interaction as an atmospheric analogy to the functionality of a multiport liquid-propellant rocket engine injector. The results showed that electric field–induced ionic winds were capable of improving flame stability by extension of the lean flammability limit and increased blowoff velocity. Single-burner configurations closer to the anode wall had more significant effects on the flame response due to stronger electric fields generated at those locations. The cylindrical anode was more effective in changing the flame response due to larger surface area, leading to higher field strengths. It has been concluded that a system with multiple flames enhances the effects of applied electric fields, which seems to indicate the potential to effectively modify the flame response in rocket engines with multiple injection ports.

Nomenclature

a	=	electrode gap, cm
E	=	electric field, V/m
j	=	current density, A/cm^2
k	=	ionic mobility, cm^2/(V · s)
P	=	electric power, W
U	=	flow velocity, m/s
V	=	voltage, kV
ρ	=	mixture density, g/cm^3
Φ	=	equivalence ratio

I. Introduction

THE effects of an electric field on a flame have been a topic of interest since the beginning of the 19th century when Brande [1] reported a change in heat and mass transfer of a candle flame between two electrodes. Many studies [2–14] have been conducted since then to provide a better understanding of the mechanisms and characteristics of the interaction between electric fields and flames. In the experiments conducted by Payne and Weinberg [15] and Lawton and Weinberg [16] the ionic wind body-force was attributed as the driving mechanism for the observed effects the electric field caused on a flame. The ionic wind body-force is an electrohydrodynamic effect caused by electron-molecule and ion-molecule collisions, and the rate of these collisions influences the flame behavior, making it a momentum-driven process. The collisions are caused by electrostatic acceleration from the electric field between the electrodes that drives positive ions toward the cathode and negative ions and electrons toward the anode. The process of momentum transfer from these collisions is sustained for as long as a voltage difference between the electrodes exists. The ionic wind is currently the most accepted theory of how the field affects the flame. Although not directly involved in the ionic wind momentum transfer process due to their low mass, high-energy electrons can also increase the number of ionized species in the gas via collisional excitation and ionization.

The electrons are also involved in the recombination reaction with positive ions, which is the basis for an alternative explanation proposed by other authors [10,17]; the explanation suggests that the ionic wind force is not sufficient to cause the observed changes in a flame. They proposed that the flame response is instead caused by an increase in mass diffusivity and a resulting decrease of the local Lewis number of the flame. The mass diffusivity is increased by the production of light radicals from dissociative recombination of electrons and chemi-ionization–derived H_3O^+, HCO^+, and other positives ions driven to the flame preheat zone near the burner. The effectiveness of this dissociative recombination mechanism or other ion/electron chemical mechanism is still debated.

The results of various studies have shown the ability of an electric field to increase flame stability by extension of the lower flammability limit and increased blowoff velocity [2–6,11], reduce CO and NO_x emissions [13,14], and potentially suppress or modify different modes of thermoacoustic and thermodiffusive instabilities [10,12,18,19] at several different experimental conditions. Most of the experiments in the literature are conducted using a ring, grid, or rod electrode centered over a single burner nozzle or a cluster of nozzles that create a single merged symmetric flame. These simplified experimental setups make it easier to observe and understand the flame response. However, real combustion devices such as rocket engines often have multiple injectors that would be offset from any central electrode. Additionally, the geometry and operating conditions of rocket combustion chambers make integration of a downstream central electrode problematic structurally and many cause unwanted flow field disturbances. An alternative for the central electrode is a cylindrical electrode that surrounds the flame that could be integrated into the walls of the combustion chamber itself. Tube- or cylinder-type electrodes have been studied in the past [20–28], though also with single central flames. With multiple injectors and thus multiple flames, the location relative to the electrode/chamber walls becomes a factor in the electric field strength and thus effect on the flame. For potential real-world application of electric field control of engines, the effect of asymmetry of the flame and electrode needs to be examined. In rocket engines, electric fields could modify the location and rate [17] of heat release in the combustion chamber with the potential for suppressing combustion instabilities [4,5,10,29,30], lessen heat flux to injector and chamber walls, and reduce required chamber dimensions for complete combustion [17]. Other applications include increasing or suppressing [21,31] the burning rate of propellant grains in solid rocket motors, which could be used for thrust management and control.

Received 16 August 2016; revision received 25 July 2017; accepted for publication 27 July 2017; published online 31 August 2017.

*Graduate Research Assistant, Propulsion Research Center, 301 Sparkman Dr. Student Member AIAA.

†Assistant Professor, Mechanical and Aerospace Engineering, 301 Sparkman Dr. Senior Member AIAA.

In this work, we investigated the effects of an applied direct current (DC) electric field on two burner configurations consisting of a single burner at different locations and a simplified multielement burner inside a large cylindrical electrode, both operating with a lean, premixed methane-air flame at atmospheric conditions. The use of DC electric fields versus microwave, RF, or pulsed DC is preferred due to the simplicity of steady DC and the ease of scaling with pressure [14].

The effects of the DC electric field on the lean flammability limit and blowoff velocity of the single- and multielement burner are compared. The goal was to understand how the different element locations and the potential for flame interaction affect the electric field–induced effects as an atmospheric analogy for multi-injector liquid rocket engines (LREs). Numerical simulations of the electric fields using finite-element software were also done to provide further insight into the physics.

II. Experimental Setup

The experimental setup, shown in Fig. 1, consisted of a brass manifold with four outlet ports from which four burners could be installed, a cylindrical anode opened on both ends, and a DC high-voltage power supply with a maximum voltage of 10 kV. Steel wool was packed into the manifold to ensure a uniform and evenly distributed flow in all four burners. Figure 2 shows an example picture of the multielement burner flame. The flames are similar in shape and size with slight variations due to ambient perturbations or slight flow variations between the burners from flow inhomogeneity in the manifold. These differences and perturbations did not affect the flame response through repeated tests. The manifold and burners were grounded and functioned as the cathode in the system, whereas the cylinder acted as the anode. A 1-MΩ high-voltage resistor was connected between the high-voltage power supply and the anode to measure the current. A lean ($\Phi = 0.80$), premixed methane-air mixture was fed into the manifold and burners, and the volumetric flow rate of each gas was controlled by MKS mass flow controllers as depicted in Fig. 1.

Two different anodes were used to characterize the flame behavior in this work, a stainless steel cylinder and a copper ring. This choice of anodes was used to understand the effect of increased anode surface area on the flame response. The larger-surface-area cylinder should have more field lines, for a given voltage, and thus a larger effect on the flame. The cylinder had inner and outer diameters of 162 and 168 mm, respectively, and height of 154 mm. This anode geometry was chosen with the intent of emulating a simplified rocket engine combustor. The ring had inner and outer diameters of 152 and 172 mm. The distance from the burner head to the upper rim of both anodes was 88 mm.

Fig. 2 Multielement burner flames.

Two burner configurations were tested with both the cylinder and ring anodes. The first configuration used a single 7-mm ID burner tube placed at three different radial locations, center, 40 mm, and 60 mm with both anodes. The flame blowoff velocity and lean flammability limit were determined at different applied bias voltages. Blowoff velocity tests were conducted by increasing both the air and fuel flow rate while maintaining $\Phi = 0.80$. Flammability limit tests were conducted by decreasing fuel and increasing air while holding a constant total flow rate of 2.50 SLM (standard liters per minute). The single-burner configuration established a baseline of how the electric field affects blowoff and flammability at different locations in the electric field. The second burner configuration used four burners installed 20 mm from each other as shown in Fig. 1. In the figure, Burner 1 is the centerline burner. The blowoff test conditions (i.e., $\Phi = 0.80$) remained the same for the multiple-burner tests, but the flow rate for the flammability limit tests was increased to a total of 10.00 SLM due to the increased number of burners to obtain similar flames as the single-burner configuration. The flame blowoff velocity and lean flammability limits were found for burners 1–4 to determine whether the existence of multiple simultaneous flames at different distances from the electrode had the same response to the electric field.

Numerical simulations using finite-element method magnetics (FEMM) were done to model the electric field produced by the different anode and burner configurations. The simulations were performed without the flame present as the program is unable to account for reaction chemistry. Therefore, the simulations created in

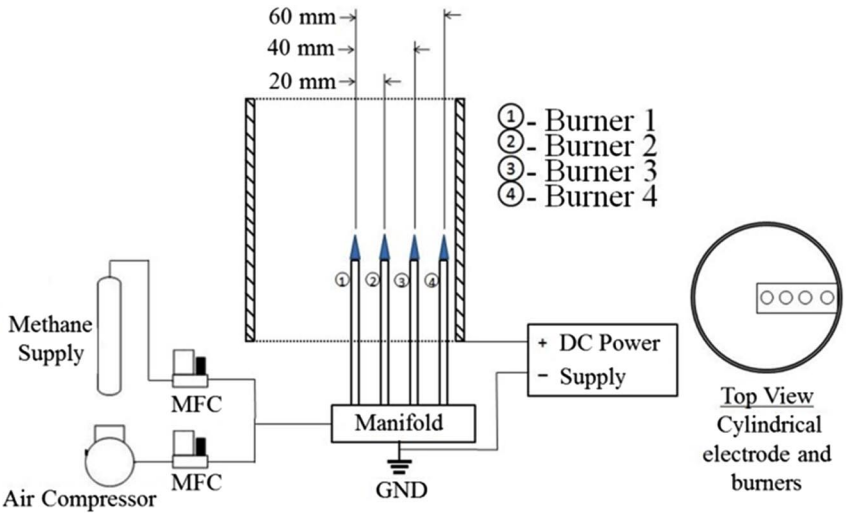

Fig. 1 Experimental setup showing a simplified multielement injection burner (grounded) and cylinder (anode).

this study only focused on predicting electric field behavior for different anode geometries and number of burners in the system. There is expected to be a difference between these field results and the actual electric field due to the presence of the electrically charged flame plasma. However, the electric field maps should provide some insight into the different behaviors observed.

III. Experimental Results

A. Electrical Measurement

The effectiveness of a flame response to an electric field depends on the electric current flowing through it [16]. The anode geometry and proximity to the flame front will determine the magnitude of the current. The most straightforward method of measuring the flame electrical characteristics is the current-voltage (I-V) curve. Figure 3 presents the I-V characteristics for the cylindrical anode with a single burner at center, 40 mm, and 60 mm, and the four-burner case. The test was conducted at $\Phi = 0.80$ and flow rates of 2.50 SLM for the single-burner cases and 10 SLM for the multielement burner. Because ion density is a function of the stoichiometry and flame area, current flow is likely to decrease in the flammability limit tests because the equivalence ratio is reduced until the flame is extinguished, and increase in the blowoff velocity tests where higher flow rates lead to large flame surface areas.

For the single-burner configuration, the magnitude of the current flowing through the flame increased as the burner moved closer toward the cylinder wall, which indicates a more effective action of the electric field [32] for these cases. According to Fig. 3, the flame response is greater for single burners that are placed near the wall. The multiple-burner configuration measured higher currents than all locations except for the single burner at 60 mm even though the multielement configuration also had a burner at 60 mm. This difference is due to an uneven distribution of the field lines between the single- and multielement burner cases due to a difference in the overall surface areas of the cathodes/burners. For the single burner, all the electron and ions flow from and to a single point, whereas they are distributed between the four burners in the multielement burner case. It is interesting to note that the total electrical power input is small ($P < 1$ W). The highest electrical power input was for the multiple-burner configuration at 0.365 W. Also, Fig. 3 shows no indication of any configuration of reaching a saturation current in the voltage ranges tested, indicating that larger changes to the flame could be obtained.

B. Lean Flammability Limit

A fuel-air mixture only ignites, and is sustained, within a specific mixture ratio between the lower and upper limits of flammability [33]. The lower limit corresponds to a leaner mixture and has an equivalence ratio smaller than unity ($\Phi < 1$), whereas the upper limit represents a richer mixture with equivalence ratio larger than unity ($\Phi > 1$). In addition to the physicochemical properties of the mixture, flammability limits also depend on experimental setup factors such as heat loss to the burner and surroundings [34]. To minimize the effects of heat losses to the system, the flammability limit study was carried out on the same apparatus and constant volumetric flow rates throughout its entirety.

1. *Single-Burner Configuration*

The lean flammability limit was determined at the three radial locations using the cylinder and ring anodes to investigate the effect of location and anode surface area on a flame. Figure 4 shows that the flame lean flammability limit decreases with the applied bias voltage on both anode geometries at all locations. The average error in Fig. 4 was calculated from a data set containing four data points for each combination of applied voltage, burner radial position, and anode geometry. The average error value ranged from 0 to ± 0.006.

The lean limit equivalence ratio for the cylindrical anode at all three locations decreased from 0.61 at 0 V to 0.46 at 5 kV, independent of the burner location (Fig. 4a). The voltage for the 40 mm and center locations was further increased to 7 and 9 kV, respectively; however, the lean limit remained unchanged, which indicates the existence of some critical limit of the electric field effect. Higher voltages were not possible due to arcing between the electrodes. The ring anode, placed

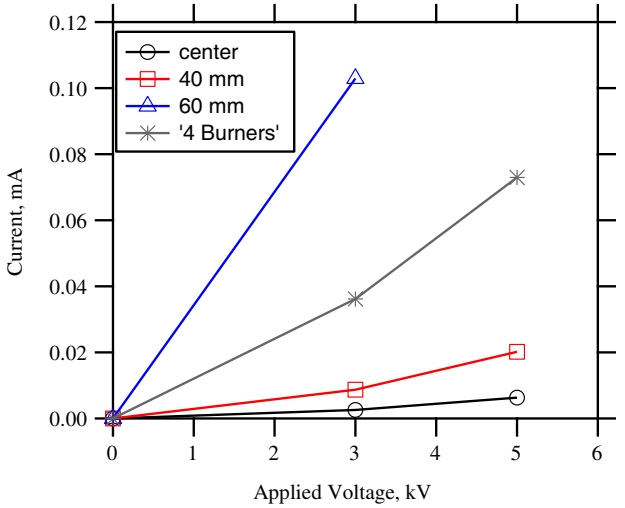

Fig. 3 Current/voltage characteristics measured for single- and multiple-burner configurations.

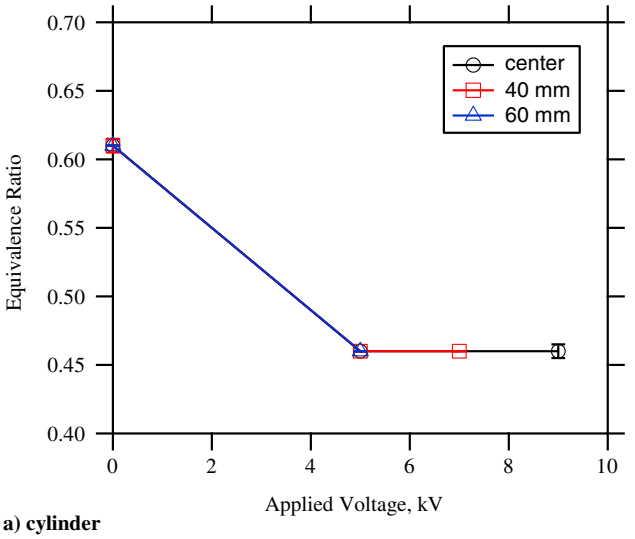

a) cylinder

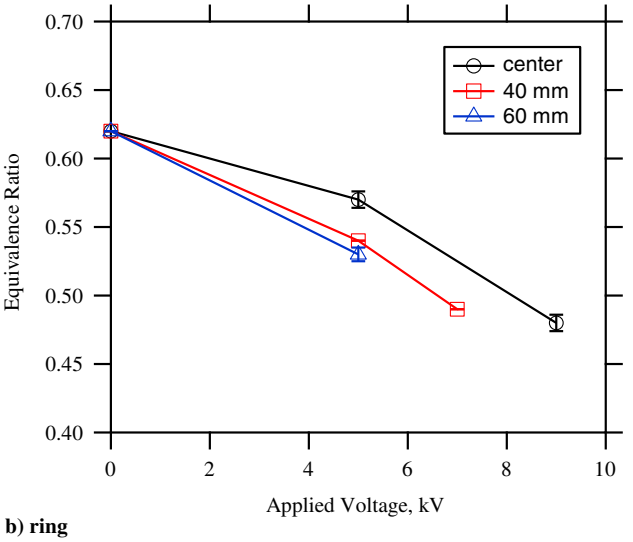

b) ring

Fig. 4 Extension of the lean flammability limit for a premixed methane-air flame using a cylinder (a) and ring anodes (b).

at the same height as the top of the cylinder, showed a smaller extension of the lean limit at 5 kV. The ring anode was also sensitive to the spatial location of the burner, unlike the cylinder anode. Flame equivalence ratio for the center burner decreased from 0.62 at 0 V to 0.56 at 5 kV. At 9 kV the equivalence ratio decreased to 0.47. The 40 and 60 mm cases showed a more significant decrease at 5 kV, from $\Phi = 0.62$ to 0.54 and 0.53, respectively.

Based on these results, it is clear that the anode surface area is a factor in the flame response. The cylindrical anode produced a stronger and more immediate effect on the flame lean limit at only 5 kV instead of 9 kV, making it a more effective geometry because a stronger flame response can be obtained with lower bias voltages.

2. *Multiple-Burner Configuration*

Because it was previously determined that the cylinder is more effective than the ring as the anode, the multiple-burner test investigated only the cylindrical anode. The multiple-burner configuration investigated the electric field effect on burners 1–4 to determine whether a combination of close proximity to the anode wall and possible flame-to-flame interaction between the burners would alter the results obtained from the single-burner measurements. Because all four burners were fed from the same manifold, the overall equivalence ratio to the manifold was continually decreased until all the flames disappeared. The equivalence ratio when each flame went out was recorded as the lean limit for that burner. Figure 5 shows that the four burners had different lean limits of flammability at a given voltage and a faster decrease was observed for burners closer to the anode wall. The average error in Fig. 5 was calculated from a data set containing three data points for each combination of applied voltage and anode geometry. The average error value ranged from 0 to ± 0.006.

The graph shows that the lean limit equivalence ratio varied for the individual burners. Burners 1, 2, and 4 decreased from $\Phi = 0.60$ at 0 kV to 0.48 at 5 kV, whereas burner 3 dropped to $\Phi = 0.46$ at the same voltage. In the single-burner cylinder anode configuration, the lean flammability limit was insensitive to the radial location of the burner, all reaching $\Phi = 0.46$ at 5 kV. Larger extensions were gradually obtained for burners closer to the anode wall at 3 kV. Up to this voltage, burners 3 and 4 had the same lean limits. The converging of the lean limit equivalence ratio to 0.48 at 5 kV for burners 1, 2, and 4 indicates a critical limit of the electric field effect, as it was seen for the single-burner configuration.

C. Blowoff Velocity

Flame stability is achieved when the local flame speed matches the local flow velocity. Blowoff and liftoff conditions occur when the flow velocity exceeds the flame speed, causing the flame to detach from the burner rim and eventually extinguish. Flame speed is primarily a chemical property dependent on the mixture ratio, pressure, and temperature.

1. *Single-Burner Configuration*

Similar to the flammability limit experiment, the blowoff velocity was determined at three burner locations (center, 40 mm, and 60 mm) with both anode geometries (cylinder and ring). The blowoff velocity was calculated based on the flow of the fuel and air and the known diameter of the burners. As expected, an increase in flame blowoff velocity was achieved when the flame is subject to an electric field, a behavior observed by many other authors [5–7,11,13,14,35]. However, in this work, we see that the blowoff velocity varies with location and proximity to the anode. In contrast to the cylindrical anode results for lean flammability limit extension, the blowoff velocity changed at different radial locations, as shown in Fig. 6. With the cylindrical anode, the maximum blowoff velocity measured was roughly equal, ~ 10 m/s, for all three burner locations, but at different voltages (Fig. 6a). The closer to the wall, the lower the voltage needed. The ring anode followed the same trend that the 40 and 60 mm locations saw a greater increase in blowoff velocity with the same voltage. It is likely that the blowoff velocity could have been increased even further with higher voltages; however, the experiment was limited by the 10 kV power supply and arcing at high voltages for the 40 and 60 mm locations. Although both anodes increased the blowoff velocity, the cylindrical anode had the largest increase per voltage.

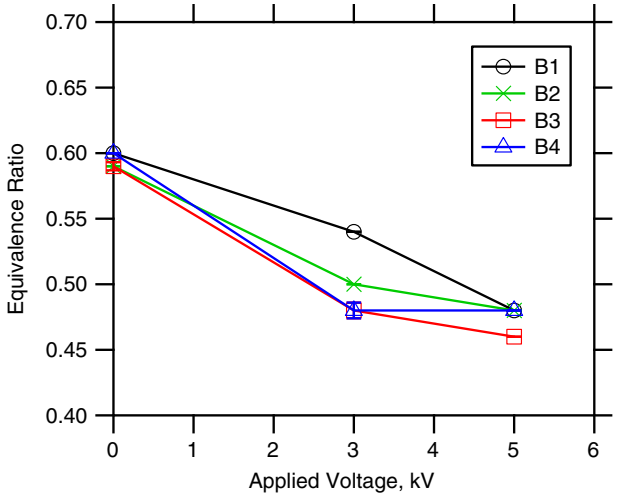

Fig. 5 Extension of the lean flammability limit for a premixed methane-air flame in a multiple-element burner.

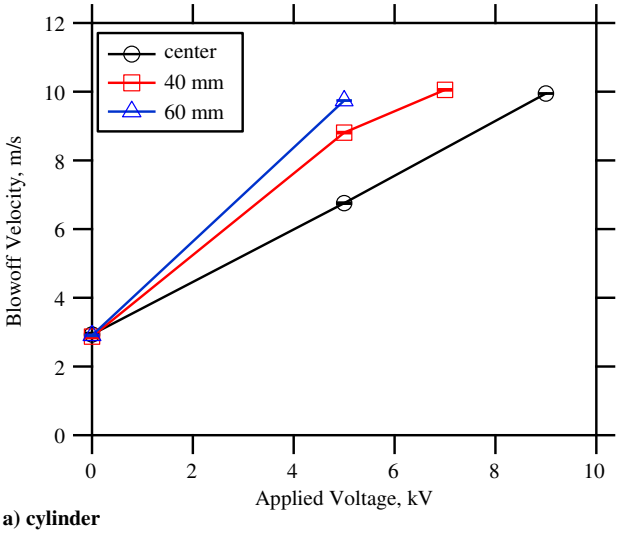

a) cylinder

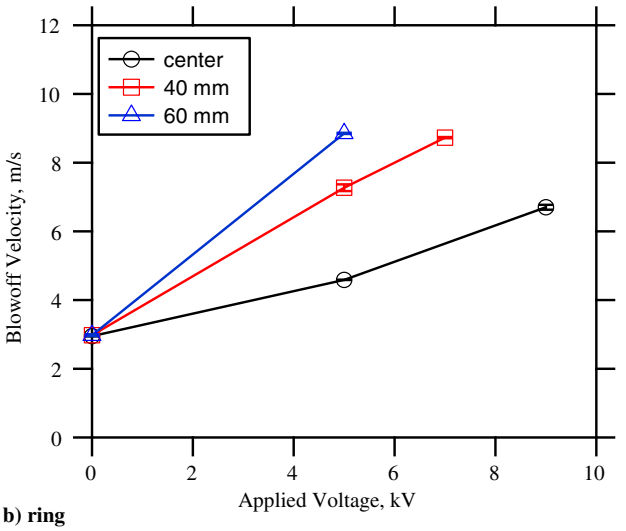

b) ring

Fig. 6 Blowoff characteristics for a premixed methane-air flame with electric field interaction on a cylinder (a) and ring anodes (b).

A direct comparison shows that the cylindrical anode causes a stronger flame response than the ring anode, similar to the lean flammability limit, thus again indicating a dependency on burner location and anode surface area. The cylindrical anode had a greater increase in blowoff velocity than the ring at all experimental conditions. The average error in Fig. 6 was calculated from a data set containing five data points for each combination of applied voltage, burner radial position, and anode geometry. The average error value ranged from 0 to ±0.10 m/s.

2. *Multiple-Burner Configuration*

For the multiple-burner tests, the blowoff velocity was measured with the assumption that the total flow rate into the manifold was evenly distributed to all four burners. Visual inspection of the flames (Fig. 2) showed flames similar in shapes and size, supporting the assumption. Figure 7 shows that the blowoff velocity is a linear function of the applied voltage and the same for all burners. The average error in Fig. 7 was calculated from a data set containing three data points for each combination of applied voltage and anode geometry. The average error value ranged from 0.14 to ±0.65 m/s. Visually, all four flames appear to blowoff at the same time once the flow rate was increased past the limit. This is a significant departure from the four-burner lean limit results and the single-burner blowoff results. Both results previously indicated that the four burners had different responses due to their location. This result indicates that something is affecting or linking the behavior of each individual burner and so they behave as a single unit, at least for blowoff.

The maximum blowoff velocity is also noticeably higher than the single-burner case. The presence of multiple flames seems to sustain each other by increasing the heat release inside of the cylinder. This behavior is evident when comparing both configurations at the 0 kV case. The blowoff velocity occurred at ∼2.90 m/s for the center, 40 mm, and 60 mm locations in the single-burner case in the single-flame case, whereas for the multielement burner this velocity was at ∼5.80 m/s.

The main advantage of the multielement burner is the lower applied voltage required for large flame responses, which directly affects the size of the power supply needed for engine applications. At 1 kV, the flame blowoff velocity was extended to ∼9.62 m/s. Similar results were obtained for the single burner at 60 mm (∼9.74 m/s) but at 5 kV. Lower voltages are also desirable to reduce the electrical power required and avoid corona and arc discharges that can damage the equipment. Higher voltage tests beyond 2 kV were not possible due to the very high flow rates needed to cause blowoff that were beyond the flow controller's capacity.

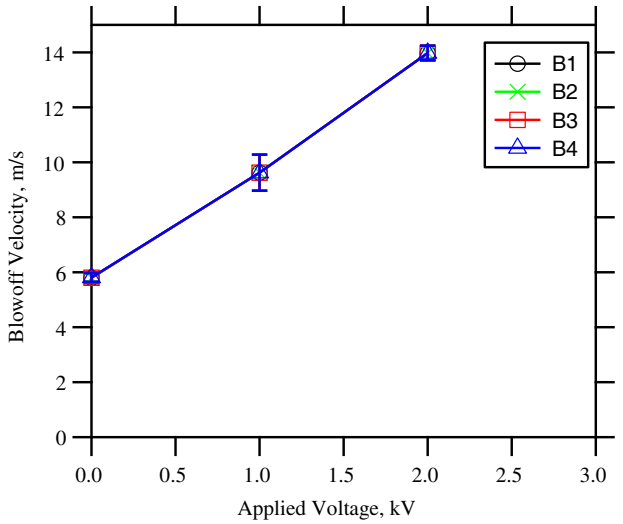

Fig. 7 Blowoff characteristics for a premixed methane-air flame in a multielement burner.

IV. Numerical Results

A 2D model of the potential field produced by the cylinder and ring anode geometries with a grounded burner was simulated with the finite-element modeling tool FEMM. The model does not take into account the presence of ions or electrons. The model results are shown in Table 1 for an applied voltage of 9 kV. The colored contours show the potential distribution and the arrows indicate the electric field (dV/dx) streamlines. Longer and larger arrows indicate larger potential gradients and thus stronger electric field lines. The electric field lines are generated radially from the higher potential electrode (anode) toward the lower potential electrode (cathode). A comparison between the single burner at 0 and 60 mm with the cylinder and ring anodes shows that the strength of electric field streamlines produced by the cylindrical anode is significantly higher than that produced by the ring anode, characterized by the larger arrows. The larger surface area of the cylinder generates a denser potential field that increases the strength and effectiveness of electric field in modifying a flame behavior.

The primary region of focus is the region above the burner lip where the flame would be. It is clear that the cylinder anode generates a larger potential gradient, which means that the flame ions experience larger electrostatic acceleration and thus greater collisional momentum transfer to neutrals. This would explain why the cylinder has larger effects on the lean flammability limit and blowoff velocity at lower voltages. The 60 mm simulation also shows significant differences in the direction of the electric field lines at the top of the burner. Whereas the ring anode shows mostly symmetric field lines irrespective of burner location, the cylinder anode has a strong asymmetry with a strong radial component near the wall. This will tend to push some flame ions radially away from the burner instead of downward toward the burner. This may explain why the blowoff velocity in Fig. 6 showed a smaller increase at 60 mm.

A third simulation investigated the electric field behavior for a four-burner configuration using the cylinder anode. Adding burners into the manifold increased the cathode surface area, causing a shift of the electric field lines and density in the region closest to the anode, shown here at the right wall. Though the cathode-anode distance is decreased for burner 4, the voltage drop is still the same, and thus stronger local electric fields are generated. It is expected that the burners closest to the anode wall will experience the largest effect of the ionic wind due to the interaction of its flames with this region of higher electric field strength and density. The strong radial component of the field for burner 4 will cause some ions to move radially inward toward burner 3. This would increase the electric forcing effect on burner 3, which would explain why burner 3 had a lower lean limit than the rest as seen in Fig. 5. In this case, burner 3's flame is affected by collisions with not only its own flame ions but also some of burner 4's ions.

V. Discussion

A. Lean Flammability Limit

As shown in Fig. 4a for the cylinder, an applied electric field caused an increase in the lean flammability limit from $\Phi = 0.61$ at 0 kV to $\Phi = 0.46$ at 5 kV independent of the radial location of the burner. Increasing the applied voltage had no further effect on the lean limit, indicating that beyond $\Phi = 0.46$ the methane concentration is too low to sustain combustion even with the cylinder anode at applied voltages up to 9 kV. A similar behavior was seen with the ring anode as seen in Fig. 4b. However, higher applied voltages were necessary to reach the same $\Phi = 0.46$ lean limit seen with the cylinder, which makes the ring a less effective anode. Also, with the ring the flame lean flammability limit showed a dependency on the radial position of the burner.

The strength of the ionic wind is based on the momentum balance [16,36] of ions and neutral particles in the flow, and it can be estimated using Eq. (1):

$$v = \sqrt{\frac{ja}{\rho k}} \tag{1}$$

Table 1 Electric field model for different anode geometries and burner configurations

Burner/anode configuration	Model	→ E, V/m
(a) Single burner/cylinder anode	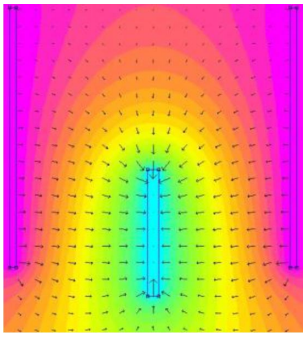	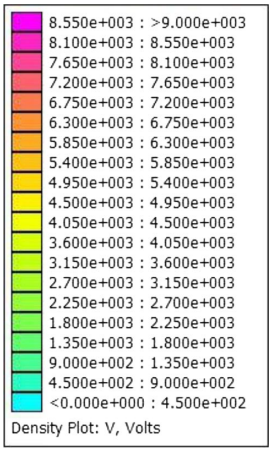
(b) Single burner/ring anode	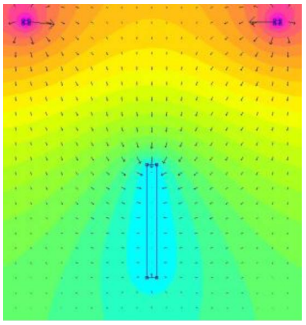	
(c) Single burner 60 mm offset/cylinder anode	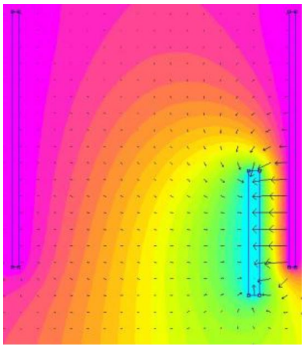	
(d) Single burner 60 mm offset/ring anode	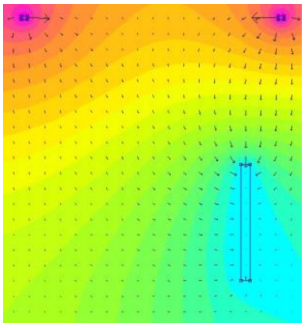	
(e) Four burners/cylinder anode	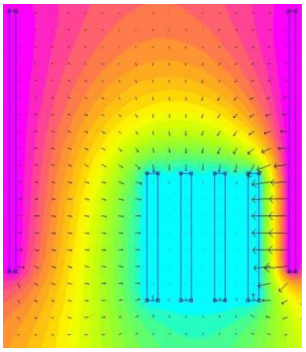	

where $j = (E^2k)/(8\pi a)$ is the current density in A/m^2, k is the ionic mobility in $m^2/(V \cdot s)$, a is the distance between the electrodes in meters, and ρ is the burned mixture density in kg/m^3. After some manipulation, the theoretical maximum velocity induced by the ionic wind can be estimated using Eq. (2):

$$v_{\max} = \frac{E}{\sqrt{8\pi\rho}} \tag{2}$$

As seen in sections (a)–(d) of Table 1, the cylinder produces larger potential gradients than the ring at both the center and 60 mm positions, which translates into stronger electric fields. The surface area of the anode was determined as the driving parameter in producing more field lines and higher field densities and, consequently, a good indicator of the electric field strength in a system for a specific anode geometry. Based on Eq. (2), stronger fields cause higher ionic velocities, making the cylinder geometry more effective in enhancing flame stability in the sense that it requires less applied voltages than the ring for the same results. The ionic wind momentum transfer explains the extension of the lean flammability limit. An applied electric field drives electrons to the anode and high-energy ions to the cathode, causing a preheating process of the fresh gas mixture. The thermal energy provided by these particles reduces the oxidation reaction activation barrier required for sustained combustion beyond the lean flammability limit as seen in Figs. 4 and 5.

The lean limit as a function of radial location with the ring and not with the cylinder is caused by effectiveness of each anode in modifying the flame response and thus the lean flammability limit at a specific voltage. At lower voltages the cylinder's large potential gradient reaches the maximum lean limit extension such that burner location has no influence. For the ring, the lower potential gradient, thus field strength, means that higher voltages are needed to reach the maximum lean limit. Additionally, moving the burner radially closer to the ring increases the electric field strength and allows a lower lean limit for a given voltage. Both the cylinder and ring anodes achieve about the same maximum lean limit of 0.46–0.47, but for the ring this limit occurs at 9 kV and for the cylinder only at 5 kV.

The multielement burner configuration was tested only with the cylindrical anode because it was found to be more effective than the ring. Figure 4 shows that increasing the applied voltage allows combustion to be sustained at lower mixture ratios. Differently from the single burner with the cylindrical anode configuration, the flames in the multielement burner extinguished at different ratios, with the burners closest to the cylinder wall having the largest decrease in the lean limits. From section (a) of Table 1, the field lines in the single centered burner in the cylinder configuration are uniform in size. As the burner is moved closer to the cylinder wall, however, the lines become nonuniform in size and thus strength. They become stronger on the right side closest to the wall and weaker on the left size. Thus the different burners exhibit different responses.

On the other hand, each burner in the multielement burner configuration experiences different field strengths. It is seen in section (e) of Table 1 that from the center burner to the one closest to the wall the electric field lines become larger, indicating the lowest and highest electric field strength for burners 1 and 4, respectively. Considering the 2D case seen in Table 1, the field lines directed to each burner are primarily dependent on the radial distance of each burner to the cylinder wall; the lines directed to burner 1 originate from the left side of the cylinder at a distance equal to the radius of the cylinder, whereas the field lines directed to burner 4 originate at a distance of only 20 mm. This is in accordance with the results seen in Fig. 5.

B. Blowoff Velocity

Figures 6 and 7 show how an applied electric field increased the threshold of the gas mixture flow velocity before a flame extinguished for the single- and multielement burner cases. Similar to the results of the lean flammability limit, it was noted that the ring anode had a smaller effect on the flame response compared with the cylinder anode, which resulted in a less significant increase in the blowoff velocity and consequently a smaller enhancement in flame stability. As discussed above and seen in Fig. 6, the cylinder surface area produces larger potential gradient and electric field lines directed to the flame, which increases the strength and action of the electric field on the flame response.

The curves from Fig. 6 show that flame blowoff velocity was dependent on the radial location of the burner for both the cylinder and ring anodes. In the lean flammability limit results (Fig. 4), only the flames in the ring configuration were sensitive to the burner radial position. We did not appear to reach a limit on the blowoff velocity as a function of the burner radial location or applied voltage. The blowoff velocity could be further increased with higher voltages. Moving the burner closer to the anode wall enhanced the effect on blowoff by increasing the field strength and thus ion acceleration and momentum transfer. Contrary to the flammability limit results, the limiting parameter in this case was the applied voltage.

As seen in Fig. 7 for the multielement burner, the blowoff velocity is not dependent on the burner radial location because all flames extinguish at the same flow velocities. The only dependency in this case is on the voltage applied. A comparison between Figs. 6a and 7 shows that the flame blowoff velocity was increased by a factor of 3.36 for the single-burner case at 60 mm and 5 kV and by a factor of 1.66 and 2.41 for the multielement burner case at 1 and 2 kV, respectively. Taken as a ratio, the single-burner blowoff velocity increased by a factor of 0.67/kV and the multielement burner by a factor of 1.6–1.2/kV. It is important to note that there was no indication that 2 kV is the maximum possible applied voltage that will increase the blowoff velocity in the multielement burner. We were limited by the flow rate capability of the mass flow controller. Besides showing a higher velocity/voltage factor, the multielement burner blowoff velocity baseline (0 kV) was already twice as high as the single-burner baseline conditions. This indicates the presence of other mechanisms acting in favor of increasing the blowoff condition and eliminating the radial burner location dependency in the multielement burner configuration that was observed for the single-burner case.

One main cause of the lack of radial dependency in the multielement burner configuration is the proximity of the burners to each other. The heat release from each individual flame provides thermal energy to the adjacent flames by convection and radiation. The mutual heat transfer allows the flames to sustain each other's combustion process by increasing the temperature and thus flame speed and providing a secondary heat source to preheat the reactants. The net result is a higher blowoff velocity with and without an applied voltage. As one or more of the burners go out due to the flame speed not being able to match that of the incoming gas, the overall thermal energy of the system decreases. At this point, the mutual heat transfer between burners decreases, which causes a decrease of the flame speed in the remaining burners followed by blow out. On the other hand, the single burners are surrounded by ambient air and heat release is quickly dissipated to the surroundings. Also, the overall flame surface area in the multielement burner configuration is larger due to multiple flames and higher flow velocities, which increases the number of ions and electrons inside of the cylinder. Because the effects of the ionic wind are caused by ionic momentum transfer, a higher ion density will lead to more significant flame responses.

Ion collisions can transfer energy into both translations and internal energy modes of fuel and air molecules. Energy into translation will affect the bulk flow velocity, which is related to blowoff, whereas internal energy affects reaction rates that are related to the lean limit. The lack of a blowoff limit at the same voltages as the lean limit indicates that the ionic wind is more effective in retarding the neutral flow velocity that preheats the reactants. This is logical given the similar masses of flame ions (HCO^+ and H_3O^+) and fuel and air molecules that preferentially transfer energy into translation. Collisions with electrons or very light particles will preferentially transfer energy into internal modes. However, in this case the electrons are accelerated downstream and thus have limited interaction with the incoming reactants.

VI. Conclusions

In this study the effect of an electric field on the response of an atmospheric, premixed methane-air flame was compared for two burner configurations using two anode geometries. The burners consisted of single- and multielement configurations to determine the difference between element radial location and flame-to-flame contact interaction as an atmospheric analogy to the functionality of a liquid-propellant rocket engine injector. Flame lean limit of flammability and blowoff velocity was determined for each burner configuration and electrode geometry at different applied voltages.

The electric field–induced ionic wind causes mass transfer of ions in the field direction. Energetic ions directed toward the burners preheat the fresh gas mixture, leading to an increase in the flame temperature and speed. The observed results showed an extension of the lean flammability limit of the flame from an equivalence ratio of 0.60 to 0.46. The blowoff velocity was increased from $\sim$2.90 m/s to a maximum of $\sim$10 m/s for the single burner and from $\sim$5.8 m/s to 14 m/s for the multielement burner. Overall, single burners closer to the anode wall had a more significant effect on the flame response than burners centered in the anode. Stronger electric fields are generated at those locations because it is a function of the distance between the anode and cathode. The higher initial blowoff velocity for the multielement burner was caused by a higher heat release from the presence of multiple flames, which enabled sustained combustion at higher flow rates. The cylinder anode was more effective in changing the flame response for a given voltage due to larger surface area leading to higher field strengths.

It has been concluded that the multielement burner and cylinder configuration was the most effective configuration tested. The multielement burner increases the combustion efficiency by increasing heat release and decreasing losses to the surroundings, and the large surface area of the cylinder provides a more efficient field distribution. This combination enhances combustion stability and reduces the voltage requirements to produce desirable flame responses.

The presence of multiple flames in a system enhances the effects of the applied electric field and so, theoretically, the techniques described here have the potential to beneficially affect the flame response in rocket engines with multiple injection ports. Actual rocket engines have complex liquid, or gaseous fuel, injection characteristics that cannot be replicated in a laboratory-scale setup. Therefore, no direct correlation can be formulated between the system used in this work and liquid rocket engines (LREs). However, scaling of combustion devices is a powerful tool with the potential to predict the performance characteristic of LREs based on smaller devices. Such scaling techniques could allow the prediction of direct current (DC) forcing effects in LREs based on much simpler and inexpensive laboratory-scale combustor. More important, the simplified setup used in this work demonstrated that the flame response is sensitive to the radial location of the burner/injector to the wall electrode. Moving forward, these simplified setup can be used to better understand the cause of these spatial response variations that can eventually help LRE implementation.

Similar techniques could be used in combustion instability studies under DC forcing. Combustion instability is always present in rocket engines, especially during development phases. Although experience has led to several ways to suppress instabilities, much is still unknown about the combustion instability process itself. Applying electric fields in the combustion chamber has the potential to suppress these instabilities and provide a method to better understand the coupling mechanisms that lead to instabilities.

Acknowledgments

This work was supported by the University of Alabama in Huntsville. The authors would like to thank the Propulsion Research Center supervisor David Lineberry and facility engineer Tony Hall for support, and Roberto Dextre, Steven Doyle, Brandon Pham, and Bradley Henderson for assistance with the experiment.

References

[1] Brande, W. T., "The Bakerian Lecture: On Some New Electro-Chemical Phenomena," *Philosophical Transactions of the Royal Society of London*, Vol. 104, Jan. 1814, pp. 51–61. doi:10.1098/rstl.1814.0005

[2] Bradley, D., and Nasser, S. H., "Electrical Coronas and Burner Flame Stability," *Combustion and Flame*, Vol. 55, No. 1, 1984, pp. 53–58. doi:10.1016/0010-2180(84)90148-2

[3] Jaggers, H. C., and von Engel, A., "The Effect of Electric Fields on the Burning Velocity of Various Flames," *Combustion and Flame*, Vol. 16, No. 3, 1971, pp. 275–285. doi:10.1016/S0010-2180(71)80098-6

[4] Calcote, H. F., and Berman, C. H., "Increased Methane-Air Stability Limits by a DC Electric Field," *Proceeding ASME Fossil Fuel Combination Symposium*, 1989, pp. 25–31.

[5] Bak, M. S., Im, S. K., Mungal, M. G., and Cappelli, M. A., "Studies on the Stability Limit Extension of Premixed and Jet Diffusion Flames of Methane, Ethane, and Propane Using Nanosecond Repetitive Pulsed Discharge Plasmas," *Combustion and Flame*, Vol. 160, No. 11, 2013, pp. 2396–2403. doi:10.1016/j.combustflame.2013.05.023

[6] Kim, M. K., Chung, S. H., and Kim, H. H., "Effect of AC Electric Fields on the Stabilization of Premixed Bunsen Flames," *Proceedings of the Combustion Institute*, Vol. 33, No. 1, 2011, pp. 1137–1144. doi:10.1016/j.proci.2010.06.062

[7] Ata, A., Cowart, J. S., Vranos, A., and Cetegen, B. M., "Effects of Direct Current Electric Field on the Blowoff Characteristics of Bluff-Body Stabilized Conical Premixed Flames," *Combustion Science and Technology*, Vol. 177, No. 7, 2005, pp. 1291–1304. doi:10.1080/00102200590950476

[8] Saito, M., Sato, M., and Sawada, K., "Variation of Flame Shape and Soot Emission by Applying Electric Field," *Journal of Electrostatics*, Vol. 39, No. 4, 1997, pp. 305–311. doi:10.1016/S0304-3886(97)00127-7

[9] Marcum, S. D., and Ganguly, B. N., "Electric-Field-Induced Flame Speed Modification," *Combustion and Flame*, Vol. 143, Nos. 1–2, 2005, pp. 27–36. doi:10.1016/j.combustflame.2005.04.008

[10] Wisman, D. L., Marcum, S. D., and Ganguly, B. N., "Electrical Control of the Thermodiffusive Instability in Premixed Propane-Air Flames," *Combustion and Flame*, Vol. 151, No. 4, 2007, pp. 639–648. doi:10.1016/j.combustflame.2007.06.021

[11] Noorani, R. I., "Effect of Electric Fields on the Blowoff Limits of a Methane Air Flame," *AIAA Journal*, 1985, Vol. 23, No. 9, pp. 1452–1454. doi:10.2514/3.9108

[12] Kuhl, J., Jovicic, G., Zigan, L., Will, S., and Leipertz, A., "Influence of Electric Fields on Premixed Laminar Flames: Visualization of Perturbations and Potential for Suppression of Thermoacoustic Oscillations," *Proceedings of the Combustion Institute*, Vol. 35, No. 3, 2015, pp. 3521–3528. doi:10.1016/j.proci.2014.08.026

[13] Most, D., Hammer, T., Lins, G., Branston, D. W., Altendorfner, F., Beyrau, F., and Leipertz, A., "Electric Field Effects for Combustion Control–Optimized Geometry," *International Conference on Phenomena in Ionized Gases*, 2007, pp. 1863–1866.

[14] Sakhrieh, A., Lins, G., Dinkelacker, F., Hammer, T., Leipertz, A., and Branston, D. W., "The Influence of Pressure on the Control of Premixed Turbulent Flames Using an Electric Field," *Combustion and Flame*, Vol. 143, No. 3, 2005, pp. 313–322. doi:10.1016/j.combustflame.2005.06.009

[15] Payne, K. G., and Weinberg, F. J., "A Preliminary Investigation of Field-Induced Ion Movement in Flame Gases and Its Applications," *Proceedings of the Royal Society*, Vol. 250, No. 1262, 1959, pp. 316–336. doi:10.1098/rspa.1959.0066

[16] Lawton, J., and Weinberg, F. J., "Maximum Ion Currents from Flames and the Maximum Practical Effects of Applied Electric Fields," *Proceedings of the Royal Society*, Vol. 277, No. 1371, 1964, pp. 468–497. doi:10.1098/rspa.1964.0035

[17] Wisman, D. L., Marcum, S. D., and Ganguly, B. N., "Electric-Field-Induced Dissociative Recombination at the Base of Premixed Hydrocarbon/Air Flames," *43rd Joint Propulsion Conference & Exhibit*, AIAA Paper 2007-5672, July 2007, pp. 1–8.

[18] Kadowaki, S., "The Effects of Heat Loss on the Burning Velocity of Cellular Premixed Flames Generated by Hydrodynamic and Diffusive-Thermal Instabilities," *Combustion and Flame*, Vol. 143, No. 3, 2005,

pp. 174–182.
doi:10.1016/j.combustflame.2005.05.012

[19] Van Den Boom, J. D. B. J., Konnov, A. A., Verhasselt, A. M. H. H., Kornilov, V. N., De Goey, L. P. H., and Nijmeijer, H., "The Effect of a DC Electric Field on the Laminar Burning Velocity of Premixed Methane/Air Flames," *Proceedings of the Combustion Institute*, Vol. 32, No. 1, 2009, pp. 1237–1244.
doi:10.1016/j.proci.2008.06.083

[20] Rosocha, L. A., Kim, Y., Anderson, G. K., Lee, J. O., and Abbate, S., "Decomposition of Ethane in Atmospheric-Pressure Dielectric-Barrier Discharges: Experiments," *IEEE Transactions on Plasma Sciences*, Vol. 34, No. 6, 2006, pp. 2526–2531.
doi:10.1109/TPS.2006.886085

[21] Pantelleev, A. F., Popkov, G. A., Tsarichenko, S. G., and Shebeko, Y. N., "Effect of an Electric Field on the Flame Propagation over a Solid Material Surface," *Combustion, Explosion, and Shock Waves*, Vol. 28, No. 3, 1992, pp. 244–246.
doi:10.1007/BF00749636

[22] Kono, M., Carleton, F. B., Jones, A. R., and Weinberg, F. J., "The Effect of Nonsteady Electric Fields on Sooting Flames," *Combustion and Flame*, Vol. 78, Nos. 3–4, 1989, pp. 357–364.
doi:10.1016/0010-2180(89)90023-0

[23] Gulyaev, G. A., Popkov, G. A., and Shebeko, Y. N., "Effect of a Constane Electrical Field on Combustion of a Propena-Butane Mixture Wit Air," *Combustion, Explosion, and Shock Waves*, Vol. 21, No. 4, 1985, pp. 401–403.
doi:10.1007/BF01463407

[24] Gulyaev, G. A., Popkov, G. A., and Shebeko, Y. N., "Synergism Effects in Combined Action of Electric Field and Inert Diluent on Gas-Phase Flames," *Combustion, Explosion, and Shock Waves*, Vol. 23, No. 2, 1987, pp. 170–172.
doi:10.1007/BF00748624

[25] Payne, K. G., and Weinberg, F. J., "A Preliminary Investigation of Field-Induced Ion Movement in Flame Gases and Its Applications," *Proceedings of the Royal Society*, Vol. 250, No. 1262, 1959, pp. 316–336.
doi:10.1098/rspa.1959.0066

[26] Mitchell, J. E., and Wrigth, F. J., "Effects in Diffusion Flames by Radial Electric Fields," *Combustion and Flame*, Vol. 13, No. 4, 1969, pp. 413–418.
doi:10.1016/0010-2180(69)90111-4

[27] Panteleev, A. F., Popkov, G. A., Shebeko, Y. N., Tsarichenko, S. G., and Gorshkov, V. I., "Effect of an Electric Field on the Flame Propagation Over a Solid Material Surface," *Combustion, Explosion, and Shock Waves*, Vol. 27, No. 1, 1991, pp. 22–24.
doi:10.1007/BF00785349

[28] Panteleev, A. F., Popkov, G. A., Shebeko, Y. N., and Tsarichenko, S. G., "Effect of ac Field on the Limiting Blowoff Flow Rate Value for a Diffusion Propane-Hydrogen Flame," *Combustion, Explosion, and Shock Waves*, Vol. 29, No. 1, 1993, pp. 32–33.
doi:10.1007/BF00755324

[29] Wisman, D. L., Ganguly, B. N., and Marcum, S. D., "Importance of Electrode Location on Flames Modified by Low Applied Electric Fields," *46th AIAA Aerospace Sciences Meeting and Exhibit*, AIAA Paper 2008-1397, 2008, pp. 1–10.

[30] Altendorfner, F., Kuhl, J., Zigan, L., and Leipertz, A., "Study of the Influence of Electric Fields on Flames Using Planar LIF and PIV Techniques," *Proceedings of the Combustion Institute*, Vol. 33, No. 2, 2011, pp. 3195–3201.
doi:10.1016/j.proci.2010.05.112

[31] Mayo, P. J., Watermeier, L. A., and Weinberg, F. J., "Electrical Control of Solid Propellant Burning," *Proceedings of the Royal Society*, Vol. 284, No. 1399, 1965, pp. 488–498.
doi:10.1098/rspa.1965.0076

[32] Fialkov, A., "Investigations on Ions in Flames," *Progress in Energy and Combustion Science*, Vol. 23, Nos. 5–6, 1997, pp. 399–528.
doi:10.1016/S0360-1285(97)00016-6

[33] Turns, S. R., *An Introduction to Combustion: Concepts and Applications*, 3rd ed., Laminar Premixed Flames, McGraw–Hill, New York, 2012, Chap. 8.

[34] Law, C. K., and Egolfopoulos, F. N., "A Unified Chain-Thermal Theory of Fundamental Flammability Limits," *24th Symposium (International) on Combustion*, Vol. 24, No. 1, Elsevier, 1992, p. 1119.

[35] Altendorfner, F., and Beyrau, F., "Technical Feasibility of Electric Field Control for Turbulent Premixed Flames," *Chemical Engineering & Technology*, Vol. 33, No. 4, 2010, pp. 647–653.

[36] Lawton, J., Mayo, P. J., and Weinberg, F. J., "Electrical Control of Gas Flows in Combustion Processes," *Proceedings of the Royal Society of London A: Mathematical, Physical and Engineering Sciences*, Vol. 303, No. 1474, 1968.

J. R. Brophy
Associate Editor